N82-13691

COMPARISON OF CLOSED LOOP MODEL WITH FLIGHT TEST RESULTS

Frank L. George
Air Force Wright Aeronautical Laboratories

Introduction

The analysis presented here is part of a larger effort to develop an analytic technique capable of predicting the landing characteristics of proposed aircraft configurations in the early stages of design. In this first analysis, a linear pilot-aircraft closed loop model is evaluated using experimental data generated with the NT-33 variable stability in-flight simulator. The pilot dynamics are modeled as inner and outer servo loop closures around aircraft pitch attitude, and altitude rate-of-change respectively. The landing flare maneuver is of particular interest as recent experience with military and other highly augmented vehicles has shown this task to be relatively demanding, and potentially a critical design point. A unique feature of the pilot model used here is the incorporation of an internal model of the pilot's desired flight path for the flare maneuver.

Model Development

Data from Ref. 1 suggests the landing flare maneuver can be modeled as a closed-loop tracking task, as pictured in the following sketch.

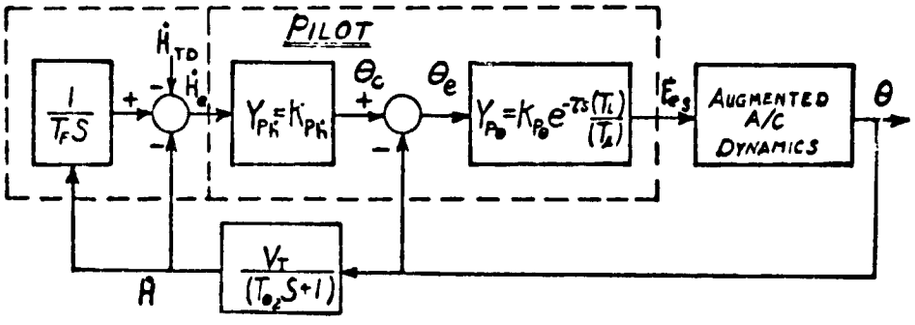

Everything inside the dotted box in this model pertains to the pilot. The pilot model is partitioned into two parts. The left hand part represents the pilot's internal model of the flare maneuver, and provides the basic error signal for tracking. This part of the model will be discussed more in following paragraphs. The right hand part of the model includes all the pilot dynamics which, as will be discussed below, consist of two gains and a time delay, plus possible first order lead or lag compensation.

As can be seen from the sketch, this model only considers pitch axis dynamics and assumes linearized small perturbation equations. The following

variables are pertinent to the discussion.

θ	- rad.	Aircraft Pitch Attitude
$\dot{H}$	- m/sec.	Altitude rate of change, or vertical velocity of aircraft
$\dot{H}_{TD}$	- m/sec.	The pilot's desired vertical velocity at touch-down
$\dot{H}_e$	- m/sec.	Error in desired vertical velocity as perceived by pilot
$1/T_F$	- 1/sec.	Flare model inverse time constant
$K_{p_{\dot{h}}}$	- rad sec/m	Pilot's internal gain to convert $\dot{h}_e$ to an attitude command
θ_c	- rad	Pilot's internal estimate of attitude required to correct $\dot{h}_e$
θ_e	- rad	Error between desired and actual aircraft attitude; as perceived by pilot
K_{p_θ}	- m/rad.	Pilot's internal gain to convert θ_e to an elevator (pitch) control motion
τ	- sec.	Pilot's delay time; approximates internal processing plus neuromuscular delays
T_L	- sec.	Pilot's optional lead compensation time
T_l	- sec.	Pilot's optional lag compensation time
Fe_s	- N	Pilot's pitch control force

As suggested in Ref. 1, the pilot's internal flare model, mentioned above, can be represented as a first order exponential. In other words, as a linear relationship between $\dot{H}$ and H, depicted in the following phase plane sketch,

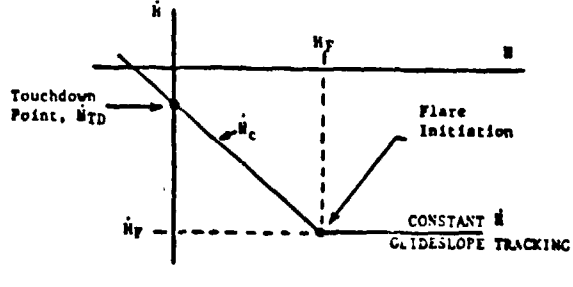

define the pilot's desired sink rate along the flare trajectory as $\dot{H}_c$, where

$$\dot{H}_c = 1/T_F \, H + \dot{H}_{TD}$$

and $1/T_F$, the inverse time constant of the corresponding exponential decay is:

$$1/T_F = \frac{\Delta\dot{H}}{\Delta H} = \frac{\dot{H}_{TD} - \dot{H}_F}{0 - H_F} .$$

Data from Ref. 2 will be used to test the model described above. For the experiment described in Ref. 2, characteristics representative of modern fighter aircraft with augmented dynamics were modeled in the variable stability NT-33. A series of ILS approaches was flown using a nominal glideslope of .044 rad (2.5 degrees); each approach was concluded with a visual flare and landing task. The flare maneuver was initiated at a nominal altitude of 15.24m (50 feet) above ground. A sink rate of .762 m/sec. (2.5 ft/sec.) at touchdown is considered acceptable. The configuration designated as 2-7 in Ref. 2 will be used as a specific example for further discussion here. For the visual flare, it is assumed the pilot has selected a desired touchdown point on the runway so the important speed is equivalent ground speed, which for this example was 61.73 m/sec. (120 knots or 202 ft/sec.) at flare initiation. Using the definitions above, these values give the ideal flare model as,

$$\dot{H} = -.11(H + 6.92) \quad \text{m/sec.}$$

with the exponential solution,

$$H = 22.16(\bar{e}^{.11t} - .31) \quad \text{m}$$

The airplane, actuator, augmentation and feel system dynamics for configuration 2-7 of Ref. 2 were examined and it was determined that a reduced order model using only the short period and command augmentation dynamics plus feel system gain would be adequate in the frequency range of $.1 \leq j\omega \leq 20.$ rad/sec.

The final closed loop model was generated by first closing an inner loop for attitude control, and then an outer loop for altitude rate. Ref. 3 suggests bandwidth and phase angle criteria for attitude control during landing of

$$\omega_B = 1.2 \text{ rad/sec}, \quad \phi_{in}\big|_{\omega_B} = \pi/2$$

with a pure time delay of 0.3 sec. For this analysis a pilot time delay of 0.33 sec was used since this value gave a convenient first order Pade' approximate expression for linear frequency domain analysis. The pilot's time delay and any compensation introduced were lumped in the attitude loop closure. Parameters were selected for the inner loop to approach the criteria mentioned above as closely as possible, while maintaining reasonable closed loop damping, for example, $\zeta_{CL} = 0.5$. For the configuration selected, this rationale resulted in a fairly low-gain system, but it was felt this would be consistent with the pilot's desire to not overcontrol so close to the ground. Figure 1 summarizes the characteristics of the attitude closed loop with no pilot compensation considered. Continuing with the outer loop closure, and accounting for initial conditions as suggested in Ref. 3, the final closed loop flare model was,

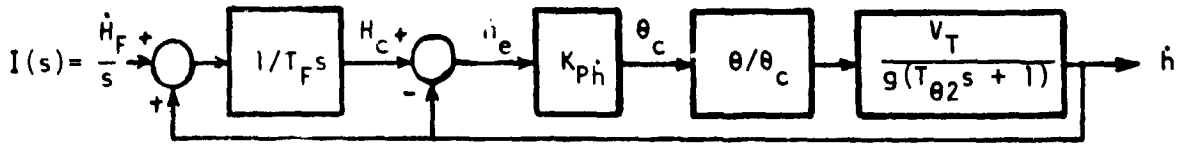

where the lower case letters are used to indicate perturbation values. The final closed loop transfer function was,

$$\frac{\dot{h}}{\dot{H}_F} = \frac{-38.61\ (S - 6)}{(S + 1.164)(S + 6.005)[S + .771 \pm j\ 1.431][S + 8.356 \pm j\ 8.611]} .$$

The forcing function for this model, using the conditions defined above, was a step scaled to represent the altitude rate at flare initiation.

Model Evaluation

Figure 2 summarizes the response characteristics of the final closed loop system, and Figure 3 compares the landing trajectories of the piloted closed loop model with an ideal exponential curve. The trajectories in Figure 3 representing the piloted system with lead and lag were generated from models developed by the same procedure as described above. The pilot lead and lag were introduced as cascade compensation within the pitch attitude loop. Figure 3 shows the pure gain and lead compensated models both result in early flares and overshoot the ideal exponential touchdown time, leading to long gliding landings which pilots might describe as "floaters". The lag compensated model, on the other hand, generally follows the exponential, but with some low frequency oscillation. An example flare trajectory from the inflight experiment is also shown on Figure 3. As the figure shows, the real flight trajectory does not follow the exponential or the analytic model path very closely except in the last 4 seconds before touchdown, where the flight trajectory is somewhat similar to the exponential. Figure 4 presents a second comparison of the flight path characteristics, using the $\dot{H}$ vs H phase plane. This presentation clearly shows the oscillatory nature of the lag compensated closed loop model. The figure also clearly shows the difference between the actual flight trajectory and the ideal exponential.

Planned Work

Further analysis of the inflight data is planned to investigate differences between the experimental and predicted flare trajectories. It is felt the closed loop model is a valid approach for the landing flare analysis because of pilot comments and the nature of observed pilot control inputs during the flare. Figure 5 shows some examples of the pilot's longitudinal control activity during flare. The experimental data will be examined to determine if significant time-varying or nonlinear characteristics are present which would account for the discrepancies with the linear, constant coefficient model.

Reference 4 investigated STOL aircraft approach and landing using the optimal control pilot model. The flare maneuver was treated as a time opti-

mal problem in that study, resulting in time varying control. An example flare trajectory from the Reference 4 results is plotted in Figure 4. Although the trajectory is rotated because of the steeper approach angle used in the STOL study, the shape generally resembles the NT-33 actual landing trajectory. This observation lends credence to the plan to extend the present investigation to consider time-varying closed loop models.

References

1. Hoh, Roger, Craig, S.J. and Ashkenas, I.L., "Identification of Minimum Acceptable Characteristics for Manual STOL Flight Path Control, Volume III Detailed Analyses and Tested Vehicle Characteristics", US DOT Report No. FAA-RD-75, 123, III, June 1976, DTIC: ADA029250.

2. Smith, Rogers E., "Effects of Control System Dynamics on Fighter Approach and Landing Longitudinal Flying Qualities, Volume I", Air Force Flight Dynamics Lab Report, AFFDL-TR-78-122, March 1978, DTIC: ADA067550.

3. Chalk, C.R., et al, "Revisions to MIL-F-8785B(ASG) Proposed by Cornell Aeronautical Laboratory Under Contract F33615-71-C-1254", Air Force Flight Dynamics Lab Report, AFFDL-TR-72-41, April 1973, DTIC: AD778489.

4. Kleinman, D.L. and Killingsworth, W.R., "A Predictive Pilot Model for STOL Aircraft Landing", NASA Langley Research Center Report, NASA CR-2374, March 1974.

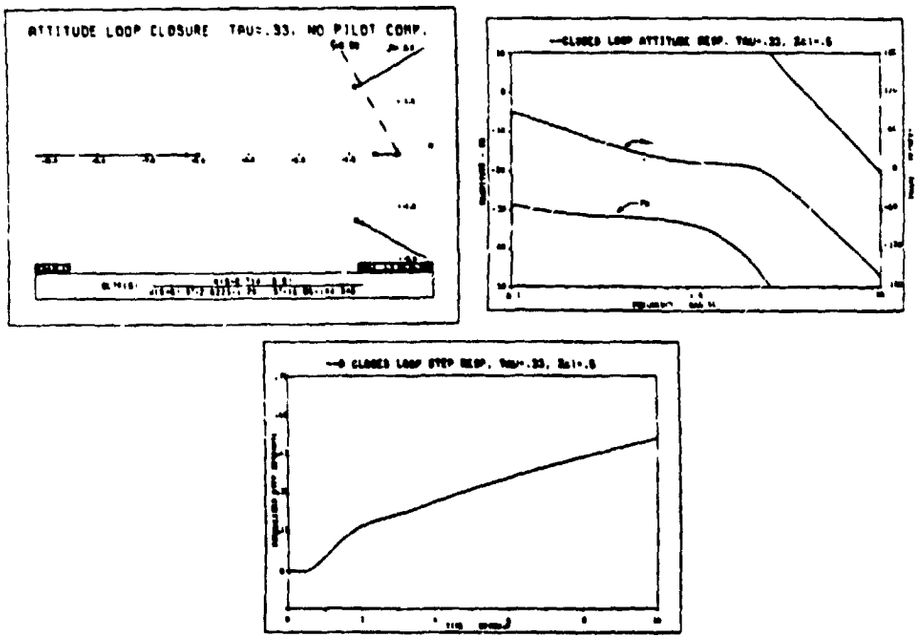

FIGURE 1. Closed Loop Attitude Response with Pure Gain Pilot

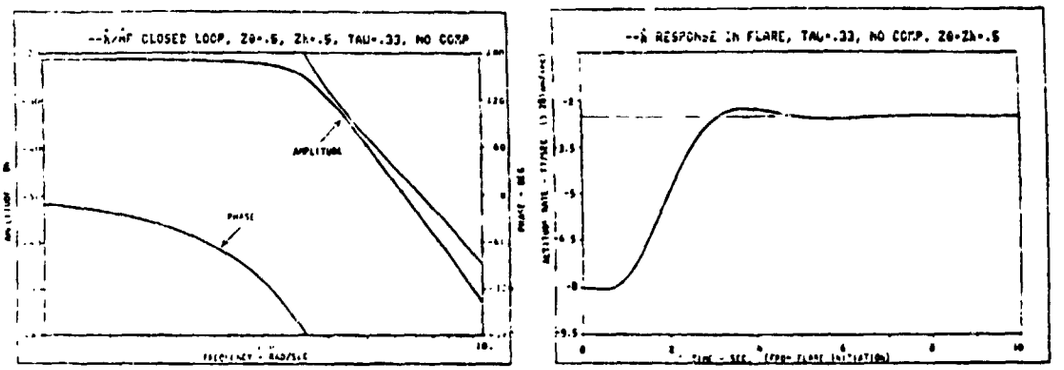

FIGURE 2. Closed Loop Flare Response with Pure Gain Pilot

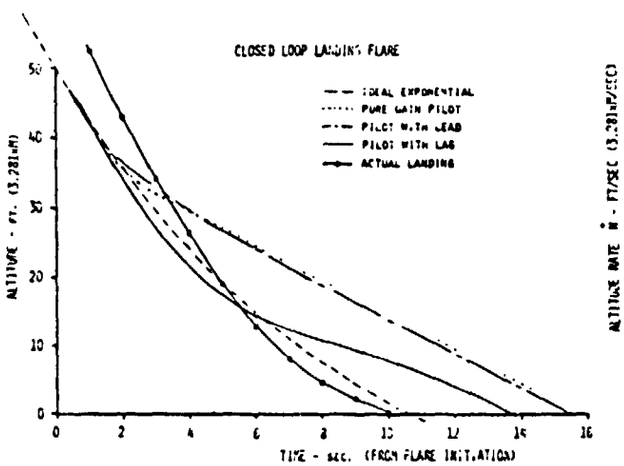

FIGURE 3. Closed Loop Flare Trajectories

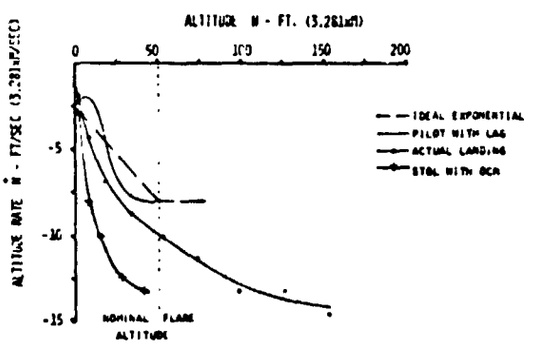

FIGURE 4. Flare Trajectory Phase Plots

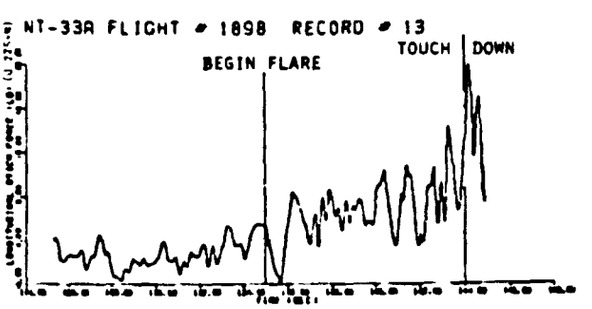

FIGURE 5. Pilot Control Inputs in Flare